Generating low frequencies: a comparison of prediction filters and well log frequency replacement

Heather J.E. Lloyd and Gary F. Margrave

ABSTRACT

Accurate bandlimited acoustic impedance inversion is impaired by the missing low-frequencies in recorded data. There are several methods for restoring these missing frequencies - they can be recorded in the field, estimated by model inversion, borrowed from well logs or predicted using the available frequencies in the spectra. Two methods of prediction filters were explored in solving for the missing frequencies. The first method is the one-lag prediction method which predicts the needed samples using one prediction filter. The second method uses multiple lags to predict the needed samples and creates a new prediction filter for each sample. These methods were tested with a simple 3-layer model and a more complicated 12-layer model where it was evident that the method was sensitive to four main parameters. The prediction methods need a reliable band of frequencies to create the filters and predict the new samples that must be flat and larger than the low-frequency gap. The length of the filter was studied and we found that the length needed to be longer than the amount of layers in the model. The third sensitivity was the effect of noise in the signal, where low signal to noise affected the character of the inversion. The fourth sensitivity was the number of layers that the method could accommodate. On a realistic synthetic example using a synthetic trace created from well logs and deconvolved both the prediction methods failed when compared with the BLIMP method. This was partially due to the natural roll-off of low frequencies when there are a large amount of layers in the model and the complication of the frequency spectrum. This study has not conclusively determined which prediction method is preferable but the one-lag method is faster and has fewer errors when compared with the multi-lag method.

INTRODUCTION

Currently most of the seismic data that is recorded in the field is bandlimited. This is partially due to the response of the earth which attenuates the signal, the lack of full frequency source output when Vibroseis sources are used, and instrumental limitations of the recording devices. This bandlimited data creates a problem when inverting for impedance as the character of the impedance is contained within the first 5 Hz of the frequency spectrum (Lindseth, 1979). While full wave inversion is not theoretically affected by the bandlimitedness of the data, acoustic inversion is still greatly affected. Methods to correct for or limit the low frequencies in bandlimited data are to record the low frequencies in the field, to use model based inversion techniques, to fill in the low-frequency gap with a well log and finally to predict the low frequencies using autoregressive prediction filters. This paper discusses two types of autoregressive prediction filters including a one-lag prediction filter and a multi-lag prediction filter.

METHOD

To help explain the importance of low frequencies in acoustic impedance inversion, a three layer model will be used. The first layer has an impedance of 1500, the second

layer has an impedance of 2500 and begins at 0.4s and the third layer has an impedance of 4000 at 1.2s. This model can be observed in the bottom panel of Figure 1. The top panel of Figure 1 shows the reflectivity of a three layer model where the bottom panel is actually the inverted impedance log using the recursion formula. This result is a perfect solution as the spectrum of the reflectivity has not been bandlimited as we can see in the top plot of Figure 2. The bottom plot in Figure 2 shows the bandlimited frequency spectrum. It can be seen that there is both a positive and negative frequency band. Figure 3 shows the bandlimited reflectivity looks like in the time in the top plot. Instead of two clean delta peaks, there are two wavelets. When we invert this reflectivity directly using the recursion formula we get the result in the bottom plot of Figure 3. The recursion formula is unable to restore the impedance when the reflectivity spectrum is bandlimited. It is evident that the missing frequencies due to the bandlimiting of the data must be replaced.

This paper was inspired by the works of D. W. Oldenburg et al (1983) where he used an autoregressive prediction method using the Burg algorithm to predict into the low-frequency gap. In this paper we have used much simpler prediction filters. The first has a lag of one and the other uses multiple lags in the algorithm. The first step of the method is to predict into the low-frequency gap using the prediction filter. Once the full spectrum has been repaired the next step would be to invert for the impedance using the recursion formula,

$$I_{j+1} = I_j \frac{1+r_j}{1-r_j} = I_0 \prod_{k=1}^{j} \frac{1+r_k}{1-r_k}, \tag{1}$$

where I represents impedance, r represents reflectivity, j is the current layer and j+1 is the next layer. A derivation can be found in Oldenburg et al. (1983) or Lloyd and Margrave (2011).

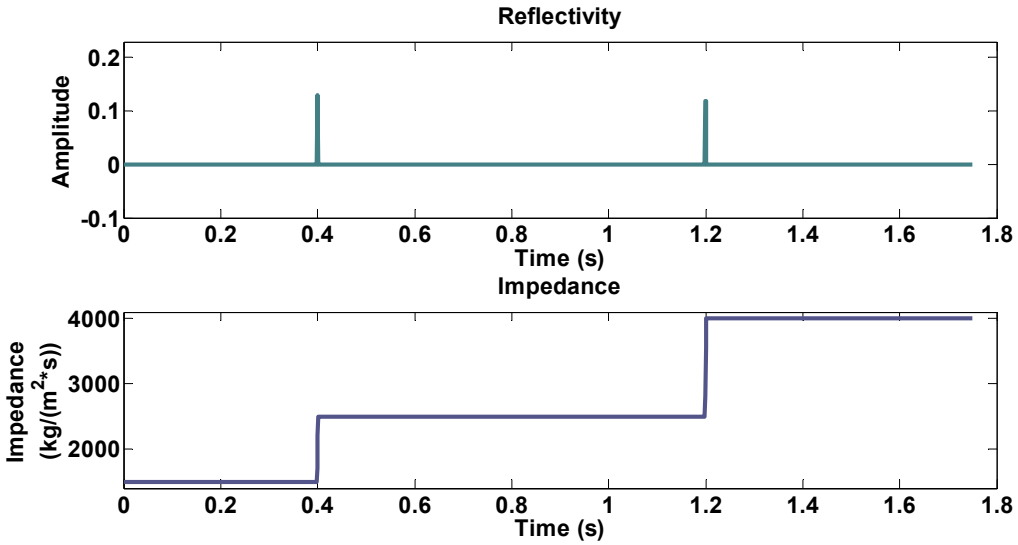

FIG 1: The reflectivity of a three layer model is shown in teal where its inverted impedance using the recursion formula is shown in blue.

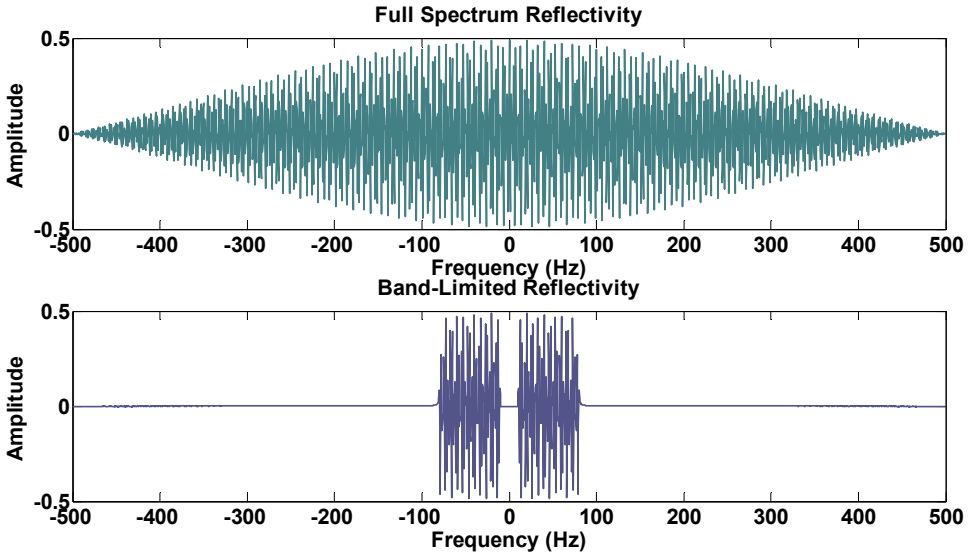

FIG 2: The full spectrum of the reflectivity is shown in the top plot in teal where the bandlimited reflectivity is shown in the bottom panel in blue. Note that there is a gap between -10 and 10 Hz caused by the bandlimited wavelet being applied to the data. All of the plots are showing the real part of the frequency spectra.

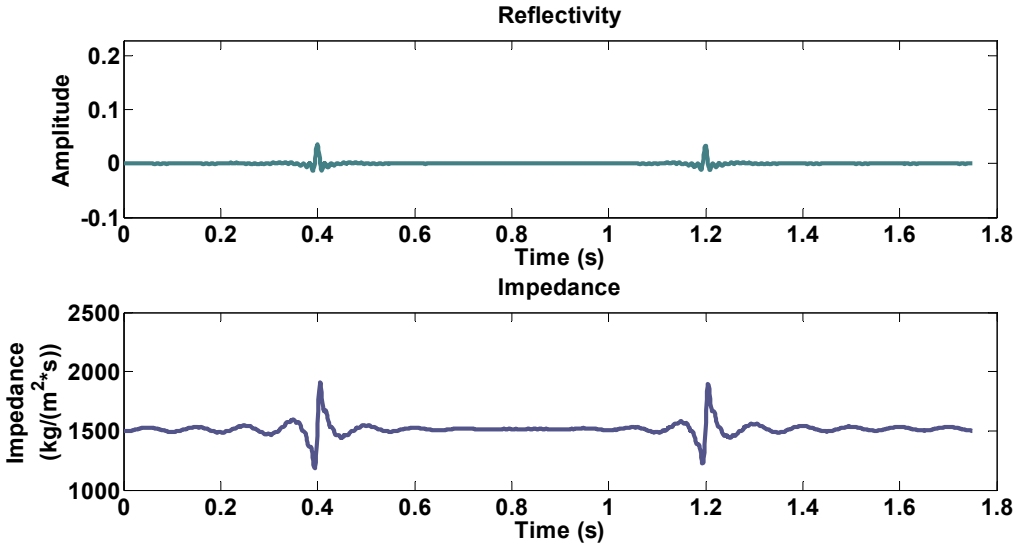

FIG 3: The bandlimited reflectivity is shown the top plot in teal and its inverted impedance is shown in the bottom plot in blue.

Prediction Filters

If we take a set of data $\mathbf{d}=[d_0\ d_1\ d_2\ ...d_m]$ and multiply it by a filter $\mathbf{a}=[a_0\ a_1\ a_2\ ..a_n]$ we get the result **c** (Claerbout,1976)

$$\begin{bmatrix} d_0 & 0 & \cdot\cdot & 0 \\ d_1 & d_0 & \cdot\cdot & 0 \\ \vdots & \vdots & \therefore & 0 \\ d_m & d_{m-1} & \cdot\cdot & d_0 \end{bmatrix} \times \begin{bmatrix} a_0 \\ a_1 \\ \vdots \\ a_n \end{bmatrix} = \begin{bmatrix} c_0 \\ c_1 \\ \vdots \\ c_m \end{bmatrix}. \tag{2}$$

If we want to create the filter from our data, **d** and solution **c,** we can solve for **a** by taking the pseudo-inverse of **d**.

$$\begin{bmatrix} a_0 \\ a_1 \\ \vdots \\ a_n \end{bmatrix} = \begin{bmatrix} d_0 & 0 & \cdot\cdot & 0 \\ d_1 & d_0 & \cdot\cdot & 0 \\ \vdots & \vdots & \therefore & 0 \\ d_m & d_{m-1} & \cdot\cdot & d_0 \end{bmatrix}^{-1} \times \begin{bmatrix} c_0 \\ c_1 \\ \vdots \\ c_m \end{bmatrix} \tag{3}$$

To create a special type of filter called the prediction filter we let **c**=[d_{0+lag}, d_{1+lag}, d_{2+lag}, ..., d_{m+lag}] and then solve for **a**.

$$\begin{bmatrix} a_0 \\ a_1 \\ \vdots \\ a_n \end{bmatrix} = \begin{bmatrix} d_0 & 0 & \cdot\cdot & 0 \\ d_1 & d_0 & \cdot\cdot & 0 \\ \vdots & \vdots & \therefore & 0 \\ d_m & d_{m-1} & \cdot\cdot & d_0 \end{bmatrix}^{-1} \times \begin{bmatrix} d_{lag+0} \\ d_{lag+1} \\ \vdots \\ d_{lag+m} \end{bmatrix}, \tag{4}$$

where lag is the amount of samples the prediction filter is predicting forward. To use prediction methods to restore the missing frequencies we need to apply this method in the frequency domain.

One-lag prediction filter method

The one-lag prediction filter can mathematically be represented by,

$$\begin{bmatrix} a_0 \\ a_1 \\ \vdots \\ a_n \end{bmatrix} = \begin{bmatrix} d_0 & 0 & \cdot\cdot & 0 \\ d_1 & d_0 & \cdot\cdot & 0 \\ \vdots & \vdots & \therefore & 0 \\ d_m & d_{m-1} & \cdot\cdot & d_0 \end{bmatrix}^{-1} \times \begin{bmatrix} d_1 \\ d_2 \\ \vdots \\ d_{m+1} \end{bmatrix}, \tag{5}$$

This method creates a prediction filter of length NL once using the useable frequency band that has not been bandlimited. This filter is then used with NL samples immediately before it to predict the next sample of the bandlimited frequency spectrum. To create the next point the filter is multiplied with the new sample plus NL-1 of the previous samples. This method is illustrated in Figure 4.

This method is applied using the positive frequency band and predicting forward into the higher positive frequencies and backward into the negative frequencies. This is repeated using the negative frequency band and predicting forward into the positive frequencies and backward into the higher negative frequencies. These results are then averaged to get

the restored frequency sequence of the reflectivity. An example of the positive and negative predictions is illustrated in Figure 5.

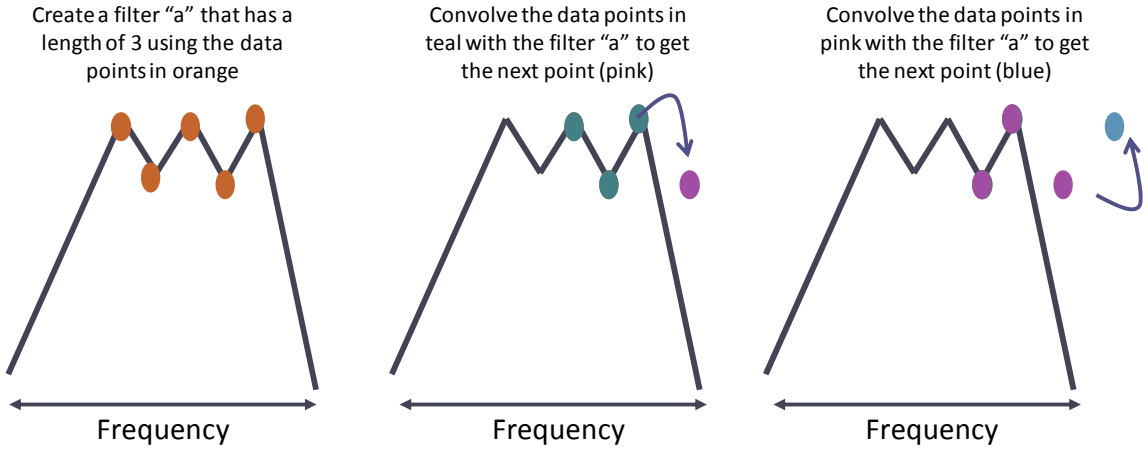

FIG 4: The one-lag prediction filter algorithm uses all the available data points in the frequency band to create a prediction filter of length NL. Once the filter is created it uses NL points and convolves with the filter to produce the next point in the frequency spectrum. The next point is calculated using NL-1 points in the frequency band plus the newly generated point to predict the next frequency point in the sequence.

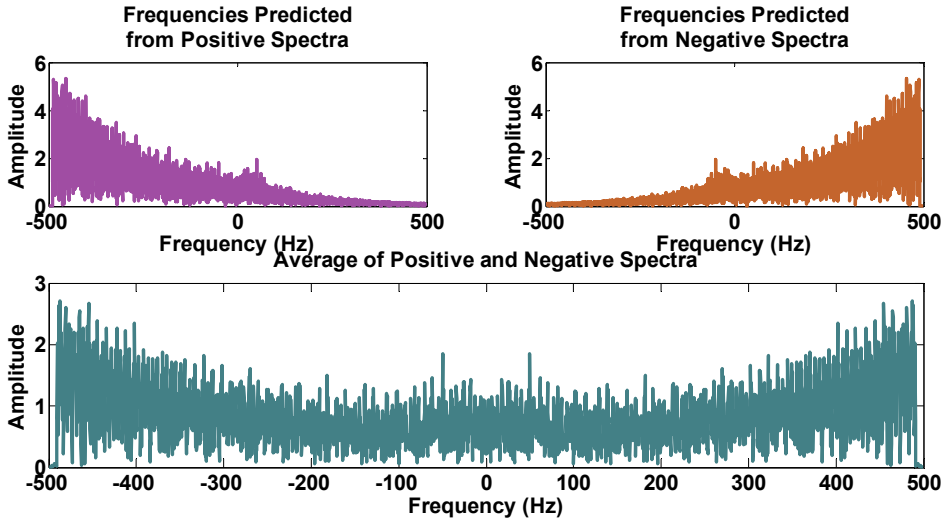

FIG 5: Both the one-lag and multi-lag algorithms predict spectra using the positive side (shown in pink) of the bandlimited spectrum and the negative side (shown in orange). These spectra are then averaged to get the full spectra of the prediction (shown in teal), note that the bandlimited gap is filled in. All of the plots are showing the amplitude spectra.

Multi-lag prediction filter method

The multi-lag prediction method works slightly differently than the one-lag method. This method creates a prediction filter for each sample that is predicted. The first sample would use all of the frequencies in the band and create a prediction filter with a lag of one

and then the filter would be multiplied with NL samples before, as in the one-lag method. The second sample requires a prediction filter that was created with a lag of two and the filter would then be multiplied with the same NL samples before, Figure 6. This continues until the lag is equal to a set percentage (default value of 20%) of the useable frequency band. When this occurs the method becomes adaptive (Claerbout 1976) as the useable frequency band is shifted such that it accommodates the newly generated samples. This method is applied in both the forward and backward directions using the positive frequency band as well as applied in the forward and backward directions using the negative frequency band. These results are then averaged as shown in Figure 5, to produce the restored frequency spectrum.

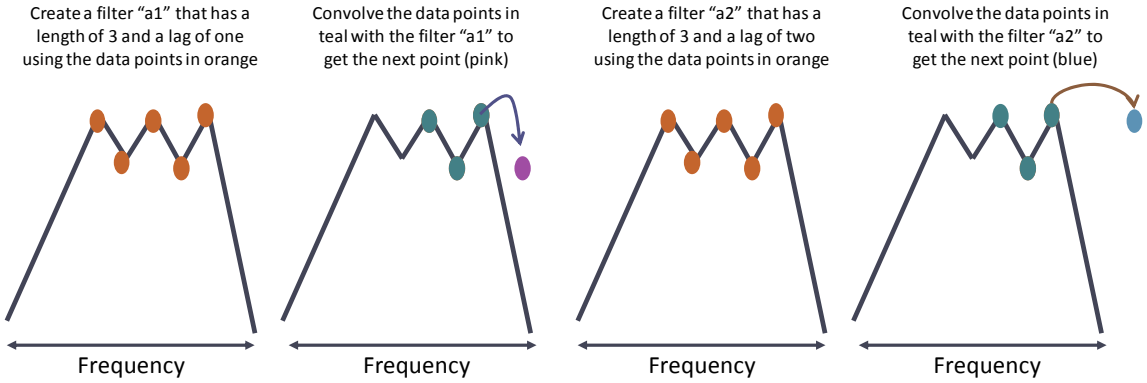

FIG 6: The multi-lag prediction filter algorithm uses all the available data points in the frequency band to create a lag 1 prediction filter of length NL. Once the filter is created it uses NL points and convolves with the filter to produce the next point in the frequency spectrum. The next point is calculated by creating a new prediction filter using a lag of 2. This new filter is then convolved with NL points to predict the next frequency point in the sequence. The cycle of creating a new filter to predict the next point is then continued for all acceptable lags.

RESULTS

To see how the two methods compare the 3-layer model shown in Figure 1 was used to test the data. Figure 7 shows the reconstruction of the reflectivity in the frequency domain. Both methods have restored most of the low frequencies which is essential to recreate the trend in the data. The method did not recreate the high frequencies accurately as the true reflectivity has a roll off for high frequencies. When we invert this data (Figure 8) we see that the impedance inversions are quite accurate with the one-lag method having a mean 4.8% error and the multi-lag method having a mean 2.2% error. This model was very simple so more complicated models will have to be investigated including a 12 layer model, without noise, with noise and with a wavelet applied, as well as a synthetic seismogram example created from a well near Hussar, Alberta.

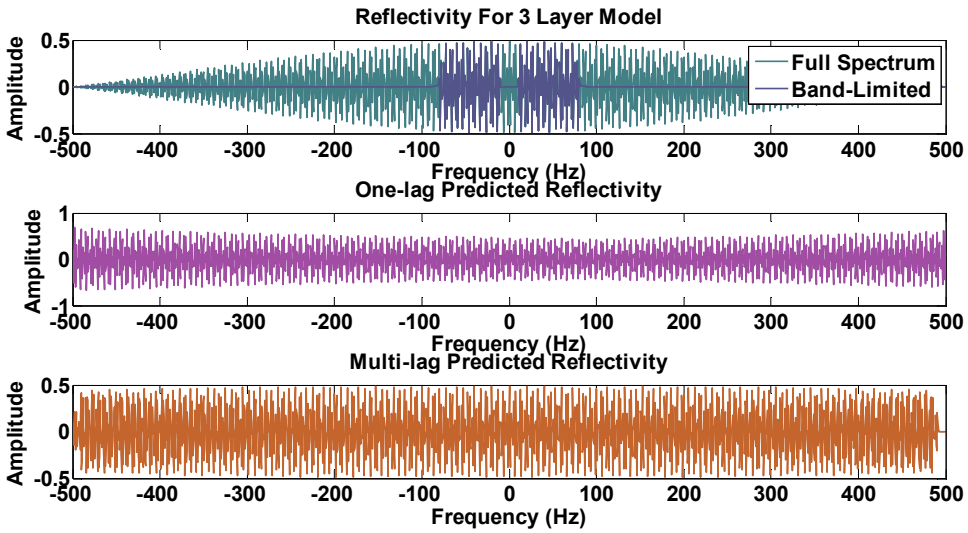

FIG 7: The top plot contains the true full spectrum of the reflectivity for a 3-layer model in teal and the bandlimited reflectivity in blue. The middle plot contains the frequency reconstruction for the one-lag predicted reflectivity in pink and the bottom plot contains the frequency reconstruction for the multi-lag predicted reflectivity in orange. All of the plots are showing the real part of the frequency spectra.

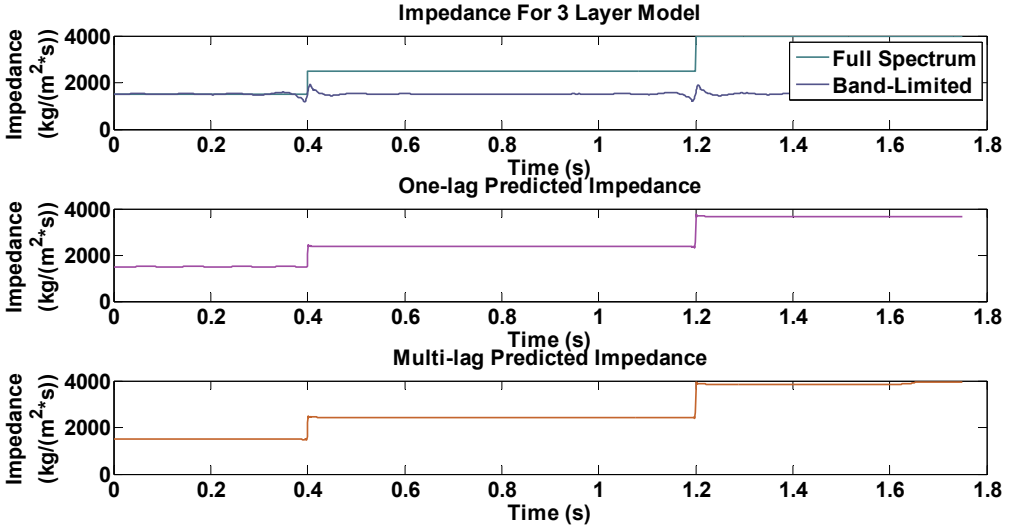

FIG 8: The inversion result using the full spectrum reflectivity (teal) can be seen in the top plot along with the inverted bandlimited reflectivity (blue). Note that the bandlimited inversion indicates where the changes in impedance should occur but lacks the changes in magnitude of the impedance. The middle plot shows the one-lag predicted impedance inversion (pink) which had a mean percent error of 4.8% where the bottom plot shows the multi-lag prediction inversion (orange) had a mean percent error of 2.2%.

Simple 12 layer model

The 12 layer model was created using random values for the impedance variations and the placement of the layers, Figure 9. The layers are of varying velocity only and the density has been ignored for this model. The impedance in this example is not always increasing like the 3-layer example so it creates a more realistic model. To have an even more realistic model, and to band limit the data, a Ricker wavelet was convolved with the reflectivity series. The real part of the frequency spectrum of the true reflectivity (teal) and the bandlimited reflectivity (blue) can be seen in the top plot of Figure 10. The shape of the bandlimited frequency spectrum has a curved trend. This produced significant problems for the prediction filter method as they would predict the low frequency roll-off from the wavelet into the gap instead of predicting the reflectivity into the gap. The reconstructions of the spectra can be seen in the middle and lower plot of Figure 10. The reflectivities were inverted to produce the impedance and the results for the impedance were undesirable as the error was high; the one-lag method had a mean error of 31% and the multi-lag method had a mean error of 30.6%. Since the Ricker example had a curved spectrum and the 3-layer example had a flat spectrum suggests that an appropriate frequency band must be chosen to create a proper reconstruction of the frequency spectrum.

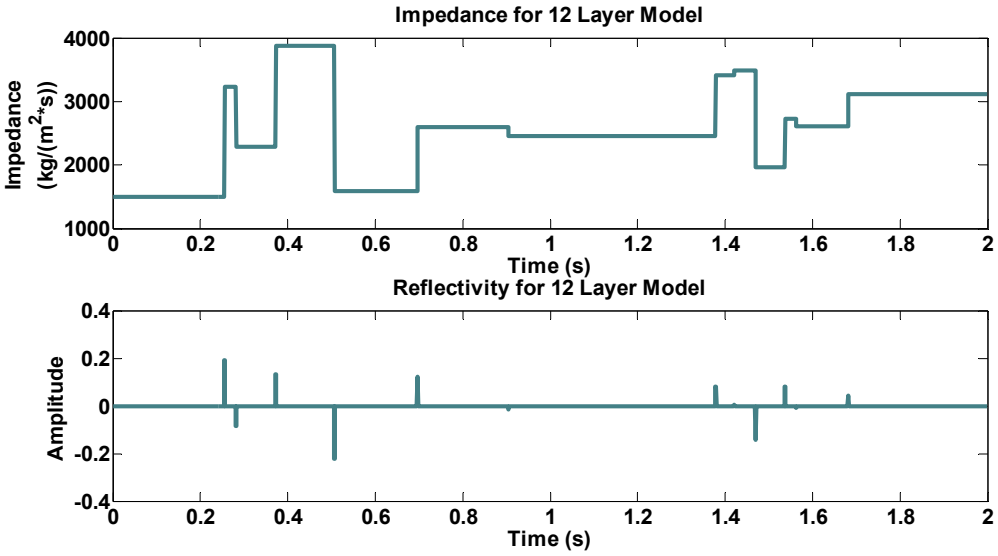

FIG 9: The impedance for the 12 layer model can be seen in the top plot where the reflectivity for the 12 layer model can be seen in the bottom plot.

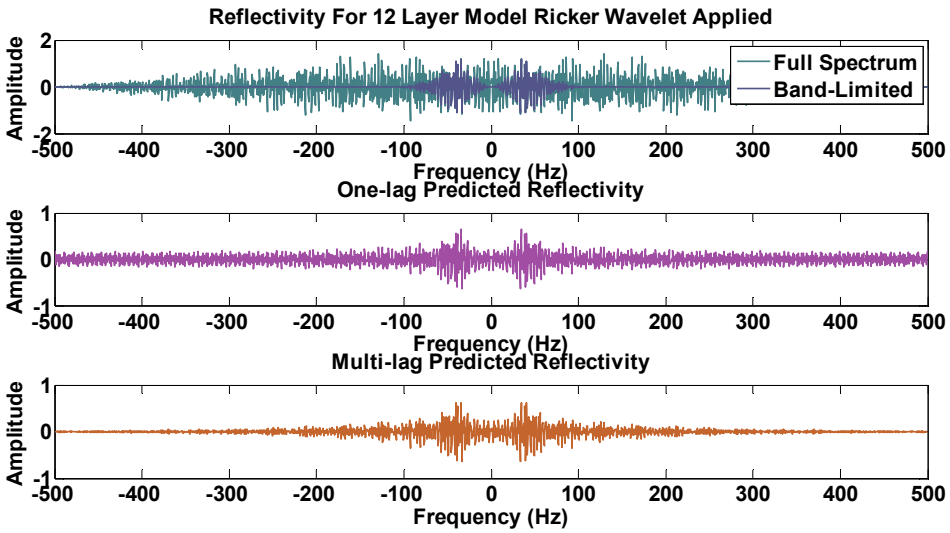

FIG 10: The true reflectivity (teal) can be seen in the top plot along with the Ricker bandlimited reflectivity (blue). The one-lag predicted reflectivity (pink) can be seen in the middle plot where as the multi-lag predicied reflectivity (orange) can be seen in the bottom plot. All of the plots are showing the real part of the frequency spectra.

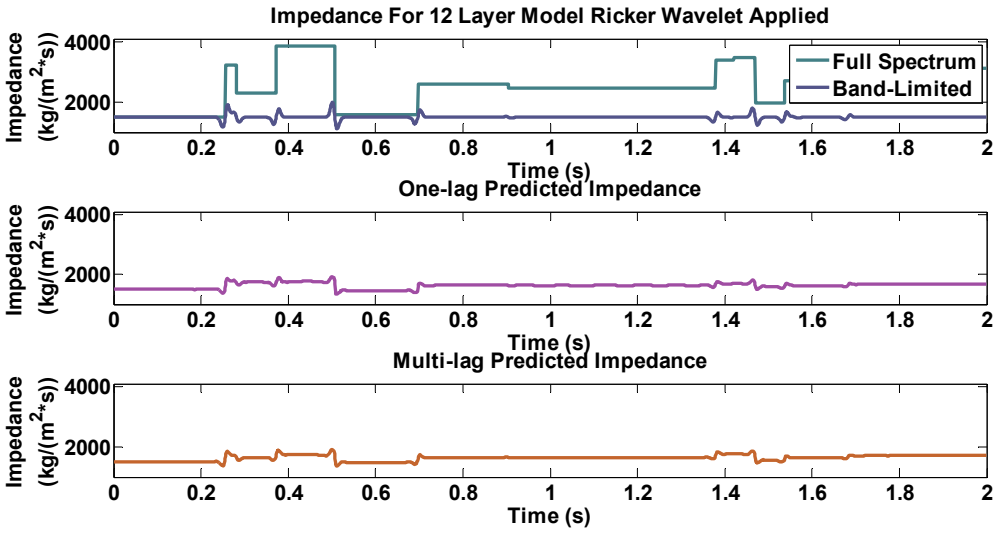

FIG 11: The true impedance (teal) can be seen in the top plot along with the inverted bandlimited reflectivity (blue). The one-lag inverted result (pink) can be seen in the middle plot where the multi-lag inverted result (orange) can be seen in the bottom plot. The error was very high for both of these results where the one-lag had a mean error of 31% and the multi-lag inversion had a slightly less mean error of 30.6%.

To choose an appropriate frequency band several tests were done on the 12 layer model with a box-car filter applied. This filter had a frequency band that hand an amplitude of 1 for samples in between 10 and 100 Hz and 0 elsewhere. Table 1 shows

the various limits of the bands that were tested. Of these choices the solution with the least error for the one-lag method was the band from 10 to 100 Hz. The multi-lag method had the least error for both impedance and reflectivity for the band from 10 to 80 Hz.

Table 1: This table shows the error associated with using different frequency cut-off values when selecting the useable part of the bandlimited spectra for the 12 layer model with a box-car filter from 10-100 Hz applied, and the length of the prediction filter (NL) was 16. The error was calculated by summing the absolute value between the true impedance and the inverted impedance.

Fmin	Fmax	One-Lag Impedance Error (10^3)	One-Lag Reflectivity Error	Multi-Lag Impedance Error (10^3)	Multi-Lag Reflectivity Error
10	60	646.28	18.32	644.64	7.80
10	80	742.15	4.42	357.98	4.19
10	100	121.47	4.35	523.28	4.45
20	60	995.39	32.87	592.23	18.07
20	80	1743.31	11.89	1355.36	5.77
20	100	785.82	6.33	464.71	4.37
30	60	2.20E+46	2.79E+04	4.93E+156	1.18E+05
30	80	1135.65	13.65	330.64	6.85
30	100	1751.94	7.24	1061.58	5.26

A curious result occurs when the band is the same width as the low-frequency gap. The error is very high as the reconstruction becomes unstable. This is true for most cases. This testing made it evident that to obtain a successful reconstruction using prediction filters the band must be flat and have no trend or curvature and be larger than the low-frequency gap that is being filled.

Another sensitive parameter is the length of the prediction filter, also referred to as NL. Table 2 shows various choices for the length of the prediction filter. Figure 12 shows the error for the impedance plotted against the length of the prediction filter. An L-curve trend can be seen from the data. Out of the values tested for NL, the best value for both methods was 24 or 36 as this produces the least error in the reflectivity and impedance. The largest error occurs for values of NL that are less than the number of layers in the model (12) and then the error levels off. The length of the prediction filter should be chosen to be larger than the number of layers in the model but less than the number of available data samples in the chosen frequency interval.

Table 2 : This table shows the error associated with using different lengths of the prediction filter (NL) for the 12 layer model with a box-car filter from 10-100 Hz applied, and the frequency cut-off values were chosen to be 10-100 Hz. The error was calculated by summing the absolute value between the true impedance and the inverted impedance.

NL	One-Lag Impedance Error (10^3)	One-Lag Reflectivity Error	Multi-Lag Impedance Error (10^3)	Multi-Lag Reflectivity Error

3	2290.76	4.09	1392.42	4.05
6	735.99	4.00	953.98	4.25
9	671.08	4.05	1142.19	9.62
12	217.98	19.96	975.64	10.71
16	233.76	14.89	370.75	8.97
18	262.86	12.16	365.58	8.33
24	281.35	10.62	253.82	8.19
36	253.69	9.74	316.76	7.26

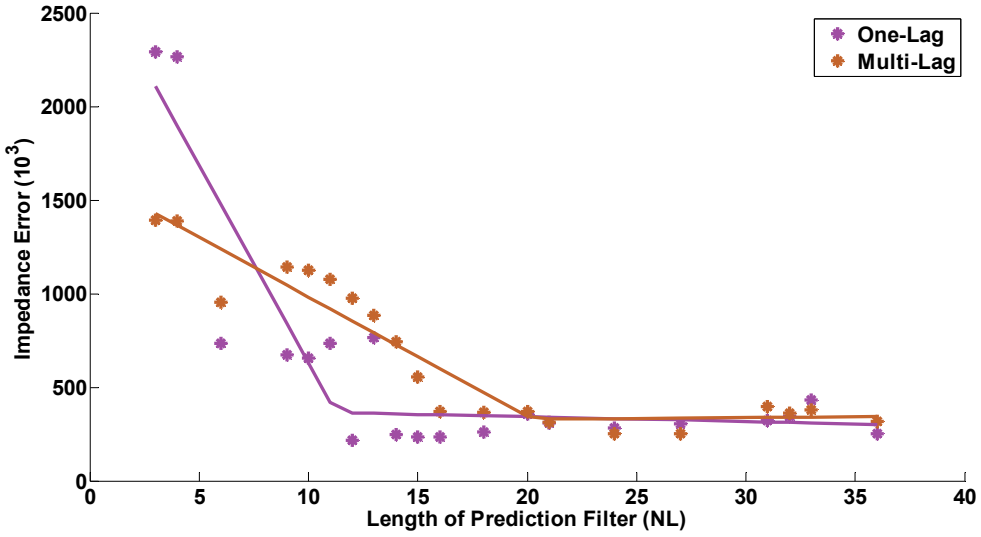

FIG 12: The impedance error plotted against the length of the prediction filter for the one-lag method (pink) and the multi-lag method (orange).

Simple 12 layer model with noise

Noise was added to the 12-layer model to see if restoring the frequency band with prediction filters was sensitive to noise. To compare the prediction methods with an alternative technique to prediction filtering the BLIMP method was chosen (Ferguson and Margrave, 1996). This method uses the low frequencies from a well log to fill in the missing low frequencies in the reflectivity spectrum. The actual impedance log was used with a low-frequency cut off of 5 Hz, so it is not surprising that the blimp method does better than the prediction results. Figure 13a shows the reflectivity of the 12-layer model with a signal to noise ratio of 0.5. The signal to noise ratio was determined by calculating the trace power in time. Figure 13b, 13c, and 13d shows the restored reflectivity for the BLIMP method, the one-lag method and the multi-lag method respectively. All of the methods are able to see through the noise and capture the reflectivity however the prediction methods do a very good job of removing the noise such that little noise is seen in the restored reflectivity. Figure 14 shows the reflectivity in the frequency domain for the BLIMP method, one-lag method and multi-lag method. Some unstable high frequencies that were introduced by the prediction filter methods needed to be truncated with a low pass filter that attenuated frequencies higher than 200 Hz. Figure 15 shows the impedance inversion for the 0.5 signal to noise case for the

BLIMP method, one-lag method and multi-lag method. The BLIMP method had 10% of the error that was incurred by the prediction filter methods. Regardless, the prediction filter methods were able to capture most of the impedance variations. This is surprising as the signal to noise ratio was 0.5 and the prediction filter methods do not require the external frequency information that the BLIMP method does. Table 3 shows the associated errors for other signal to noise ratios. When recreating figures the response of the impedance kept on changing. This shows that the prediction filter methods are sensitive to noise applied to the data. This noisy data caused some major fluctuations in the impedance which showed that the noisy data did not prefer one method over the other.

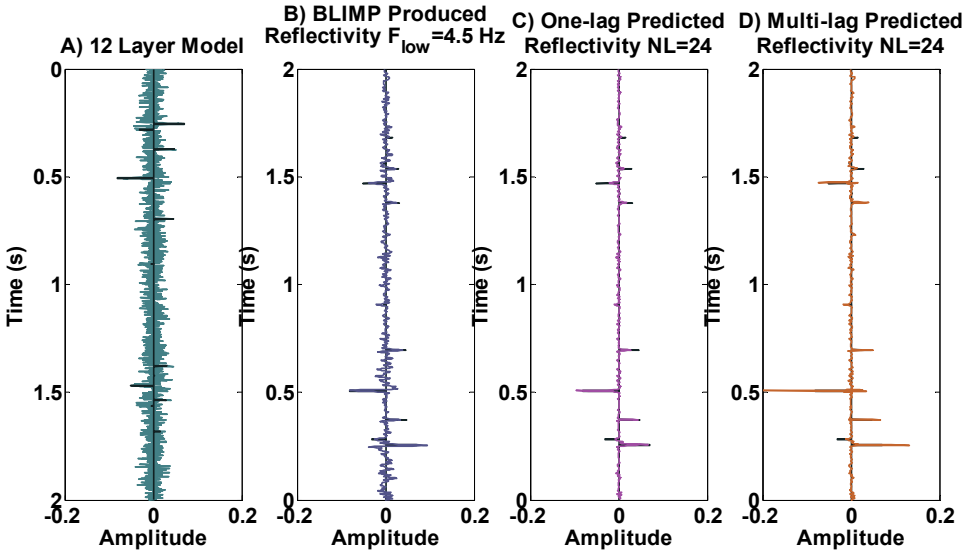

FIG 13: The signal to noise ratio was chosen to be very low, 0.5, such that the signal was almost completely hidden. The noisy signal is shown in teal with the noise free reflectivity on top in dark teal. The BLIMP inversion shown in blue had a reflectivity error of 5.7. The one-lag method (pink) had a reflectivity error of 2.8 where as the multi-lag method (orange) had an error of 5.4. The errors were calculated by summing the absolute difference between the true reflectivity and the restored reflectivity.

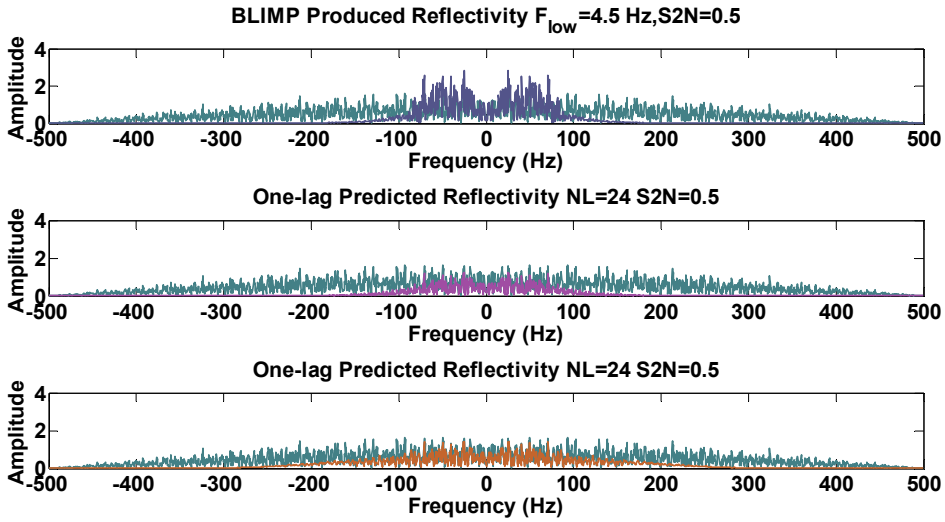

FIG 14: This shows the reflectivity restorations in the frequency domain. The teal curves represent the true reflectivity. The blue curve represents the BLIMP restored reflectivity. The pink curve represents the one-lag restored reflectivity and the orange curve represents the multi-lag restored reflectivity. Both prediction filter methods have a low pass filter applied to minimize the unstable high frequency data.

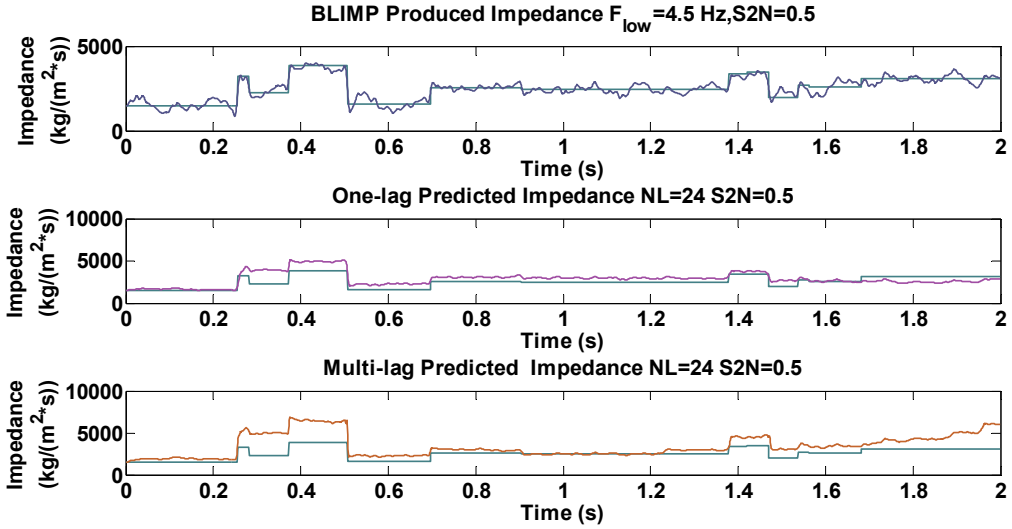

FIG 15: The inverted BLIMP impedance (blue), one-lag impedance (pink) and multi-lag impedance (orange) are plotted with the true impedance (teal). The BLIMP method has an error of 419, the one-lag method had an error of 1078 and the multi-lag method had an error of 1819. The error was calculated by summing the absolute difference between the true impedance and inverted impedance and then dividing by 1000.

Table 3: Impedance and reflectivity error for the BLIMP inversion method, one-lag prediction method and the multi-lag prediction method for noisy models using various signal to noise ratios. The 12 layer model with a box-car filter from 10-100 Hz applied was used, and the frequency cut-off values were chosen to be 10-100 Hz with NL=16. The error was calculated by summing the absolute value between the true impedance and the inverted impedance.

S2N Ratio	BLIMP Impedance Error (10^3)	BLIMP Reflectivity Error	One-Lag Impedance Error (10^3)	One-Lag Reflectivity Error	Multi-Lag Impedance Error (10^3)	Multi-Lag Reflectivity Error
0.25	263.42	11.28	3008.29	9.98	3611.10	11.63
0.5	184.89	9.79	2212.10	6.74	1482.51	6.95
1	140.20	7.61	779.09	5.00	2217.27	5.10
2	88.67	5.88	1253.97	4.78	1496.19	8.11
4	77.52	5.37	290.12	6.34	485.29	7.76
6	72.03	5.13	1026.41	21.36	1062.57	7.89
8	68.12	5.05	324.31	10.76	357.53	6.71
10	69.74	5.03	706.09	11.19	1038.04	7.83
15	70.11	4.98	551.92	16.51	745.52	11.59
20	69.32	4.95	380.19	14.05	645.97	8.55

Well-log impedance model with noise

To see if the algorithm could produce suitable results for a realistic synthetic model, a seismogram was created using the well logs from well 12-27-25-21W4 near the Hussar, AB. The well had sonic and density logs that were recorded from about 200m to 1600m. When converted to time this was only 1 second so the logs were lengthened with a linear trend to increase the sampling rate in the frequency domain. A trace was calculated using the **seismo** (CREWES, 2011) command in MATLAB using a 40 Hz minimum phase wavelet. The trace was then deconvolved both by frequency domain deconvolution and wiener deconvolution using the wavelet itself for the design operator. Figure 16 shows the amplitude spectrum of the reflectivity of the well, the seismogram with the minimum phase wavelet applied, the frequency deconvolved seismogram and the Wiener deconvolved seismogram. The amplitude spectra of the deconvolved seismograms are very white when compared to the amplitude spectrum of the reflectivity.

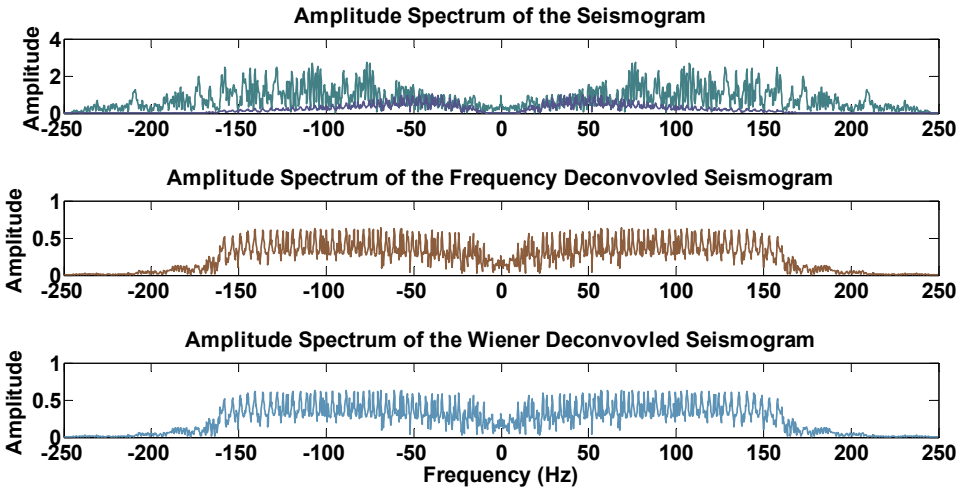

FIG 16: The amplitude spectrum of the well reflectivity (teal) and the seismogram created from the well with a minimum phase wavelet applied (dark blue) can be seen in the top plot. The middle and lower plot show the frequency deconvolved seismogram (brown) and the Wiener deconvolved seismogram (blue), respectively. Both of these spectra appear to have been over whitened.

The BLIMP method, one-lag prediction filter method and multi-lag prediction filter method were used to reconstruct the low frequencies. The frequency deconvolved data was used and a frequency band between 15 – 100 Hz was chosen. The BLIMP method used a 5 Hz low-frequency cut-off for this example. The prediction filter length was chosen to be 100. Figure 17 shows the impedance results for each method. It is obvious from this figure that the prediction filter methods were unable to reconstruct the low frequencies at all, where the BLIMP method did a satisfactory job as it is similar to the true impedance. This is illustrated again in Figure 18 where the BLIMP method has very low error when compared to the prediction filter methods. To determine if the deconvolution method has any influence on the inversion the experiment was repeated using Wiener deconvolution. A frequency band of 15 – 100 Hz and prediction length of 100 was chosen to be consistent with the frequency deconvolution results. Figure 19 shows the impedance inversion results using the BLIMP method, the one-lag prediction filter method and the multi-lag prediction filter method. Figure 20 shows the error for each method where again the BLIMP method did the best in reconstructing the impedance with the multi-lag method having only slightly less error than the one-lag method.

By comparing the two types of deconvolution on this method we can say that there is not a significant difference between the two sets of inversion results with the frequency deconvolution only having slightly better results than the Wiener deconvolution.

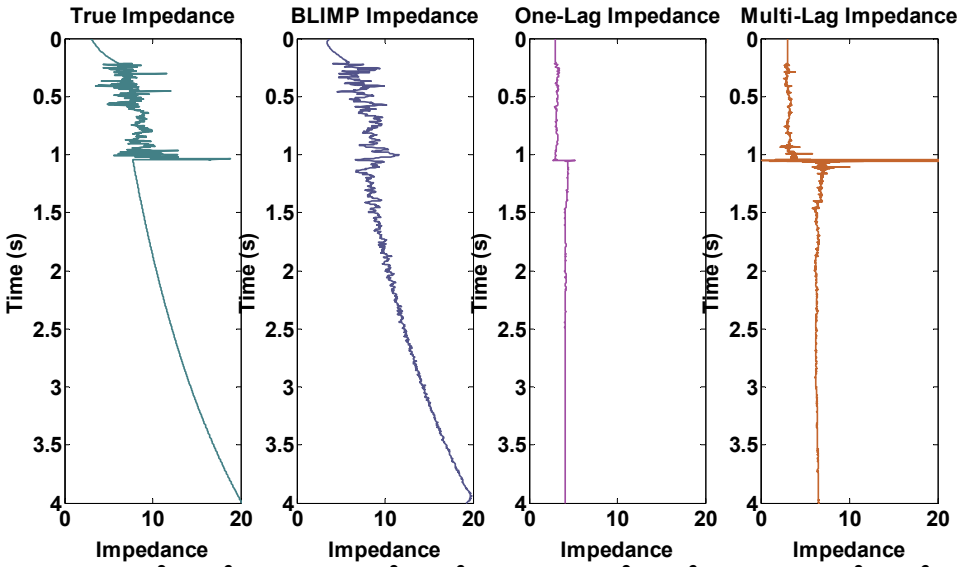

FIG 17: The impedance of the true impedance (teal), BLIMP impedance inversion result (blue), one-lag impedance inversion result (pink) and multi-lag impedance inversion result (orange) for the frequency deconvolved trace.

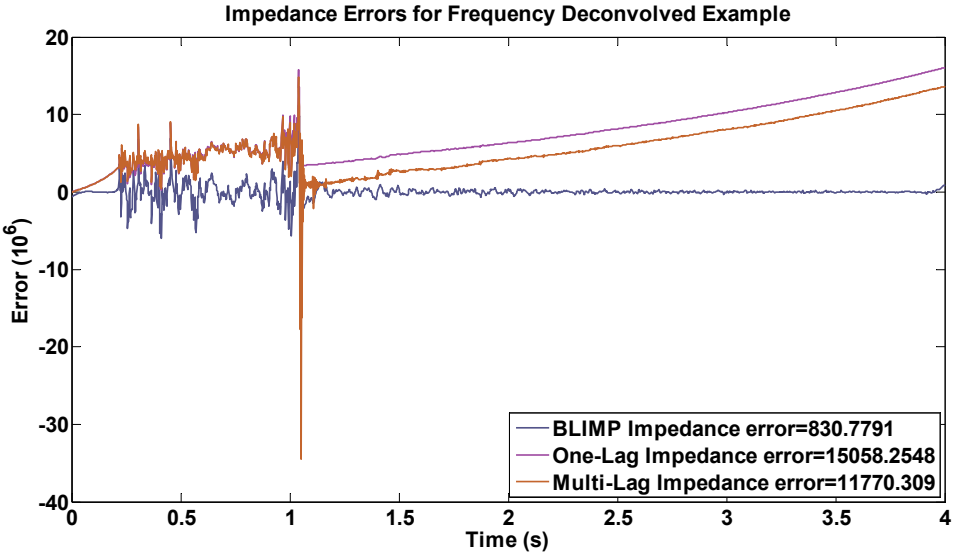

FIG 18: The difference between the true impedance and the BLIMP method (blue), one-lag method (pink) and multi-lag method (orange) was calculated. The error, calculated by summing the absolute value of the error curves, of the BLIMP method was about $831*10^6$, where the one-lag method had an error of $15058*10^6$ and the multi-lag error had an error of $11770*10^6$. This was the results using the frequency deconvolved trace.

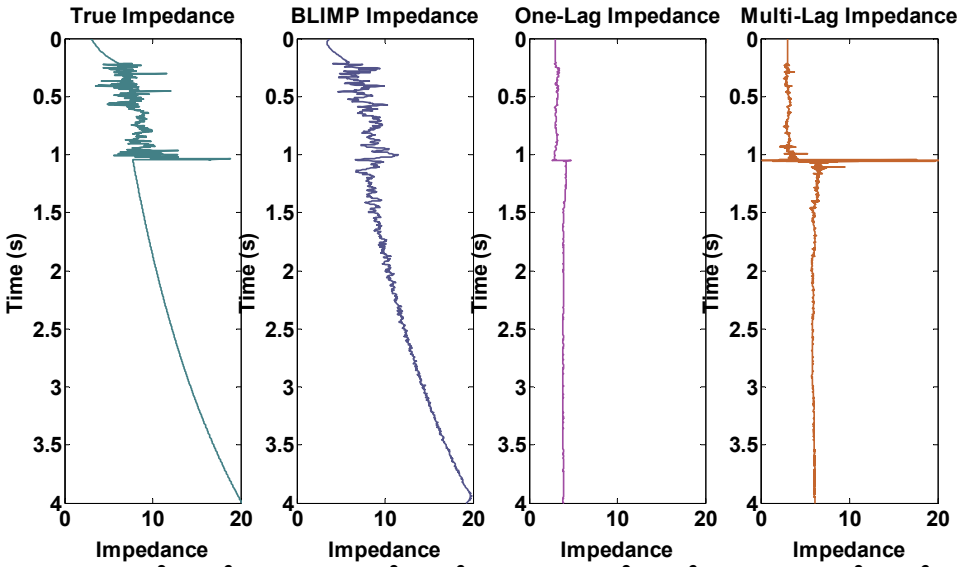

FIG 19 The impedance of the true impedance (teal), BLIMP impedance inversion result (blue), one-lag impedance inversion result (pink) and multi-lag impedance inversion result (orange) for the Wiener deconvolved trace

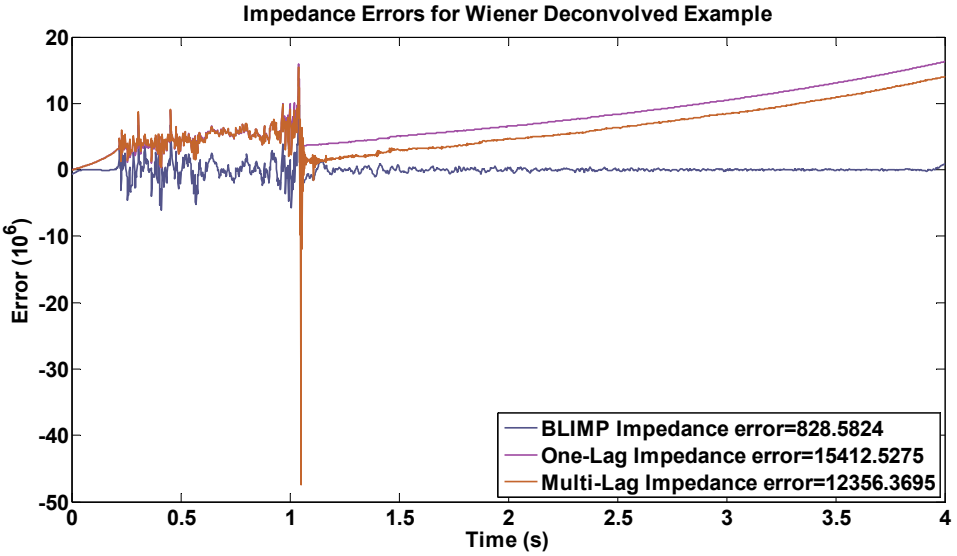

FIG 20: The difference between the true impedance and the BLIMP method (blue), one-lag method (pink) and multi-lag method (orange) was calculated. The error, calculated by summing the absolute value of the error curves, of the BLIMP method was about $829*10^6$, where the one-lag method had an error of $15413*10^6$ and the multi-lag error had an error of $12356*10^6$. This was the results using the Wiener deconvolved trace.

In Figure 16 we noticed a low-frequency notching in the amplitude spectra of the true reflectivity that did not occur in the 3-layer or 12-layer cases. Figure 21 shows the reflectivity amplitude spectra for models created with varying randomly distributed impedance layers. This figure shows that for models with less than 50 layers there is no observable roll-off in the low-frequencies. For models with 50 layers or more there is

significant notching in the low-frequencies. This curvature in the spectrum plays a part in the inability of the prediction filters to accurately reconstruct the low frequencies.

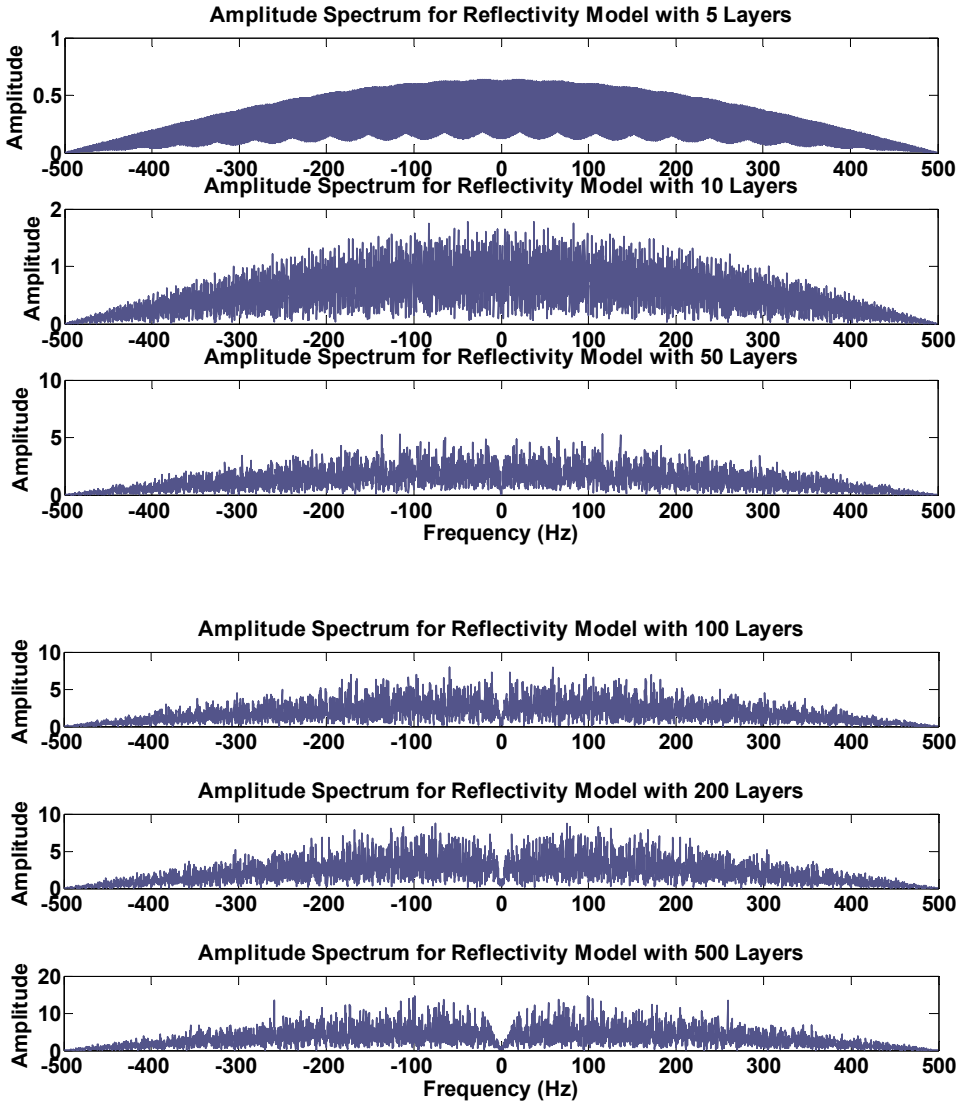

FIG 21: This figure shows the amplitude spectrum for various models created with different number of layers. As the number of layers increases the amplitude spectra begin to naturally get curvature, with the low frequencies having minimal power.

CONCLUSIONS

Several sensitive parameters became evident when doing this study. The sensitivity to curved spectra became apparent when a Ricker wavelet was convolved with the data. The prediction filters truncated the amplitude spectrum as they were following the curvature of the wavelets amplitude spectrum. To limit this effect a frequency band must be chosen that selects flat spectra. The next sensitivity was to the limits of the frequency band. After several tests, a band that selects the corners of the flat part of the wavelet's amplitude spectra produces the best results. The third sensitivity was on the length of the

filter. Significant error in the results was found when lengths of less than the number of layers in the model were used. Very large filter lengths also create a problem as the prediction takes longer but also problems arise when the filter length exceeds the amount of samples in the frequency band. The fourth sensitivity was the prediction filter's response to noise. The filters do very well when recovering the reflectivity from very noisy traces but when these are inverted it is obvious that the low-frequencies were not reconstructed properly. The noise also affects the character of the inversion so if the experiment is repeated using different noise, different impedance inversions are obtained. This is extremely sensitive when dealing with low signal to noise ratios and is less sensitive when good signals are used. The last sensitivity for the prediction filters in the response to the amount of layers in the model.

When models have a large number of layers the low-frequencies get attenuated naturally. This creates a curvature in the amplitude spectra even if there is no wavelet on the data. This is especially apparent in the well example where there is a large roll-off starting at about 100 Hz. This curvature creates significant problems for the prediction filters to be able to predict into the low frequencies as they are very sensitive to the trend and attenuate very quickly. Models with many layers also have a more complicated frequency spectrum and repeat less making it more difficult for the prediction filters to work.

When the BLIMP method was compared to the prediction filters it was obvious that the BLIMP method created results with significantly less error. This is a skewed result as the BLIMP method requires external data from impedance logs, the true impedance was used for this purpose. No conclusion can be made, whether or not there is an advantage to using the one-lag method over the multi-lag method. The one-lag method has less error associated with its impedance inversions than the multi-lag however the multi-lag generally produces better reflectivity and has flatter impedance contrasts than the one-lag method. For computational considerations the one-lag method is much faster as it only creates four prediction filters where the multi-lag method needs to create one prediction filter for each point it needs to predict. Overall it can be seen that using the current method the prediction method of recovering low frequencies is not adequate when inverting real data.

FUTURE WORK

The roll-off of the low frequencies for models with many layers creates a problem as real data has many layers and has this roll off. Methods to accommodate for this will be examined with the possibility of breaking the trace into smaller segments and then doing the prediction filtering.

ACKNOWLEDGMENTS

The authors would like to thank Kris Innanen for the direction of this paper as well as the CREWES sponsors for their interest and continued financial support of this project.

REFERENCES

Claerbout, J. F., 1976 Fundamentals of geophysical data processing: McGraw-Hill Inc., p. 130-139.
CREWES, 2011, CREWES Toolbox for MATLAB: Department of Geoscience, University of Calgary.

Ferguson, R. J. and Margrave, G. F., 1996, A simple algorithm for bandlimited impedance inversion: CREWES Research Report, Vol. 8, No. 21.

Lindseth, R. O., 1979, Synthetic sonic logs – a process for stratigraphic interpretation: Geophysics, Vol. 44, No. 1.

Lloyd, H. J. E. and Margrave, G. F., 2011 Bandlimited impedance inversion: using well logs to fill low-frequency information in a non-homogenous model: CREWES Research Report, Vol. 23, No. 21.

Oldenburg, D. W., Scheuer, T., and Levy, S., 1983, Recovery of the acoustic impedance from reflection seismograms: Geophysics, Vol. 48, No. 10.